

Electric Vehicle Charging Station Pricing Control under Balancing Reserve Capacity Commitments

Mladen Čičić, Guillaume Gasnier, Carlos Canudas-de-Wit

Abstract—Electric vehicle charging stations are expected to become key players in the future sustainable power system. We propose a framework for using them to provide balancing services to the grid, by implementing charging price control laws that ensure they are able to deliver their committed balancing capacity. The control laws are based on a simplified linearization of the Coupled Traffic, Energy, and Charging (CTEC) model, incorporating electric vehicle routing and charging decisions based on the charging price and EV state of charge. Charging stations compete with each other and must ensure a certain number of charging vehicles to maintain their role as frequency containment reserves. The results demonstrate the effectiveness of the proposed pricing control scheme in maximizing charging station profits, without violating their balancing reserve capacity commitments.

I. INTRODUCTION

The increasing prevalence of electric vehicles (EVs), encouraged by governmental policies for incentivizing EV adoption and charging infrastructure development [1], will have a substantial effect on the power system, as well as the transportation system operation. At the same time, the surge of intermittent renewable energy sources, such as wind and solar, will require an increase in balancing services to maintain grid stability [2]. Therein, battery energy storage systems are essential for providing Frequency Containment Reserves (FCR) due to their quick response time [3]. There is hope that the anticipated large EV fleet could, with appropriate charging coordination, provide these services without significantly altering their everyday routines.

Various approaches for utilizing EV charging stations for this role have been proposed, e.g. considering them as energy storage to be used for balancing the grid [4] and reducing renewable energy curtailment [5], or assimilating them into prosumers interacting with the distribution system operator in a game-theoretic context [6]. These approaches highlight the importance of considering EV charging stations as active participants in the energy system, rather than merely as passive infrastructure. Crucially, their charging prices can be used as a control input to maximize their profits [7], or respond to the balancing market [8]. Predicting the behaviour of the EVs in response to e.g. different charging price levels, is essential for charging station coordination, and the multinomial logit model [9] provides a good framework for that. This includes predicting which routes individuals will take [10], as well as when EVs decide to enter and exit a charging station [11].

Mladen Čičić, Guillaume Gasnier, and Carlos Canudas-de-Wit are with Univ. Grenoble Alpes, CNRS, Inria, Grenoble INP, GIPSA-lab, 38000 Grenoble, France (e-mail: {cicic.mladen, guillaume.gasnier, carlos.canudas-de-wit}@gipsa-lab.fr)

In this work, we propose a framework for utilizing charging stations to provide balancing services. First, in Section II, we describe the considered electromobility system and outline how charging stations are controlled to achieve our goals, using their charging prices as a control input to ensure that they can provide the contracted reserve capacity. Next, in Section III, we recall the original Coupled Traffic, Energy, and Charging (CTEC) model [12], which describes the EV traffic flows and charging dynamics. One contribution of this work is in extending the model to a general road network structure, as well as in incorporating the EV routing and charging decisions considering their State of Charge (SoC) and charging prices. Then, in Section IV, we analyse the model and design charging station pricing control laws, which is another contribution of this work. We propose a simple linear control law, and an optimization-based control law that maximizes charging station profits while ensuring that they respect their reserve capacity commitments. Finally, in Section V, the proposed control laws are tested and compared in simulations, demonstrating good performance. We conclude the paper in Section VI by summarizing its results and discussing directions for future work.

II. ELECTROMOBILITY BALANCING SERVICES

The outline of the studied electromobility system used to provide balancing services is shown in Fig. 1. We extend the CTEC model [12] to capture the effect of EV routing and charging decisions, based on their SoC and the charging prices at all charging stations in the road network. The control is executed in a decentralized manner, with each charging station choosing its price without knowing how the other charging stations' prices will change. The ability of charging stations to change their power consumption and provide FCR depends directly on the number of EVs present, causing them to compete on charging price in order to attract enough EVs to be able to satisfy the FCR requests.

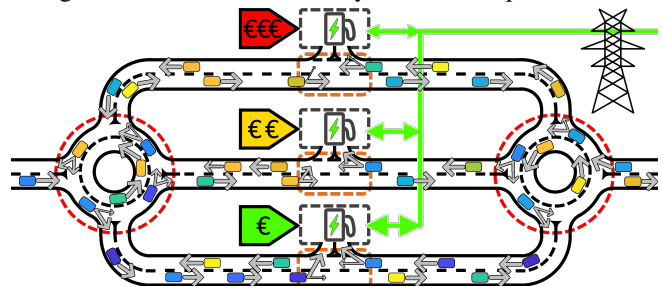


Fig. 1: Sketch of the studied electromobility system. EVs make decisions when they approach interchanges (dashed red) and charging stations (dashed orange) based on their SoC (warmer colours mean higher SoC), traffic conditions, and charging prices.

The system we study consists of three routes with road links in both directions, connecting two interchanges. At the interchanges, a portion of EVs leave the system, and constant flows of new EVs enter the system. The EVs at the interchanges then decide which of the three outwards links to take, based on the traffic conditions and charging prices, and then continue driving. At the middle of each route, there is a public charging station which EVs on the links of that route may decide to enter, based on their SoC and the charging price. After charging, the EVs continue their trips in the same direction, returning to the appropriate road link.

For each charging station $\zeta \in \mathcal{Z}$, the charging price $u_\zeta(t)$ changes with the time step of $T=1$ h, equal to the time steps of the electricity price $\pi(t)$ and FCR commitments for downward ($\mathcal{P}_\zeta^\downarrow(t) \geq 0$) and upward regulation ($\mathcal{P}_\zeta^\uparrow(t) \geq 0$), $u_\zeta(t) = u_\zeta(kT)$, $kT \leq t < (k+1)T$. Each charging station is required to change its power consumption $P_\zeta(t)$ from its nominal power $\tilde{P}_\zeta(t)$ to its prescribed regulation profile $P_\zeta^*(t)$,

$$P_\zeta^*(t) = \tilde{P}_\zeta(t) + \begin{cases} R_\zeta^\uparrow(t) \mathcal{P}_\zeta^\downarrow(t), & R_\zeta^\uparrow(t) \geq 0, \\ R_\zeta^\downarrow(t) \mathcal{P}_\zeta^\uparrow(t), & R_\zeta^\downarrow(t) < 0, \end{cases} \quad (1)$$

where $-1 \leq R_\zeta^\uparrow(t) \leq 1$ shapes the downward (\downarrow) and upward (\uparrow) balancing actions. For downward regulation, we have $R_\zeta^\uparrow(t) \mathcal{P}_\zeta^\downarrow(t) \geq 0$, i.e., the charging station needs to be able to increase $P_\zeta(t)$ (equivalent to decreasing power generation) by up to $\mathcal{P}_\zeta^\downarrow(t)$ when requested, and in case of upward regulation it must be able to decrease $P_\zeta(t)$, potentially even returning energy to the grid. If the charging station is unable to achieve $P_\zeta(t) = P_\zeta^*(t)$, it violates its FCR commitments which would incur large penalties, so the control laws must be designed in a way that makes these events rare.

III. MODEL

In this section we introduce the extended CTEC model used in this work. We first present the traffic density and SoC model on links and junctions of the network, then introduce the charging station model, and finally complete the model by discussing the decisions of the EVs.

A. Combined traffic and energy model

Consider a road network described by a directed graph $(\mathcal{J}, \mathcal{L})$, where \mathcal{J} is the set of road junctions (nodes) and \mathcal{L} the set of road links (edges). The EV traffic state on road link $l \in \mathcal{L}$, consisting of the traffic density $\rho_l(x, t)$ and SoC $\varepsilon_l(x, t) \in [0, 1]$, evolves in space x and time t according to

$$\frac{\partial \rho_l(x, t)}{\partial t} + \frac{\partial (v_l(x, t) \rho_l(x, t))}{\partial x} = 0,$$

$$\frac{\partial \varepsilon_l(x, t)}{\partial t} + v_l(x, t) \frac{\partial \varepsilon_l(x, t)}{\partial x} = \mathcal{D}(v_l(x, t)),$$

for $0 < x < X_l$, where X_l is the length of link l , given boundary conditions at $x=0$ and $x=X_l$. Here, $v_l(x, t)$ denotes the traffic speed which directly depends on the traffic density, $v_l(x, t) = \mathcal{V}(\rho_l(x, t))$, and $\mathcal{D}(v)$ is the battery discharge function, describing the rate of change of the SoC of an EV given its speed v .

For each junction $j \in \mathcal{J}$, we denote the set of links *entering* and *exiting* it by \mathcal{L}_j^- and \mathcal{L}_j^+ , respectively. Since neither vehicles nor energy can accumulate at any of the

junctions, the inflow and outflow of both are equal,

$$\sum_{l \in \mathcal{L}_j^-} q_l(X_l, t) - q_j^{\text{off}}(t) = \sum_{l \in \mathcal{L}_j^+} q_l(0, t) - q_l^{\text{on}}(t), \quad j \in \mathcal{J},$$

$$\sum_{l \in \mathcal{L}_j^-} q_l(X_l, t) \varepsilon_l(X_l, t) - q_l^{\text{off}}(t) \varepsilon_l^{\text{off}}(t) = \dots$$

$$= \sum_{l \in \mathcal{L}_j^+} q_l(0, t) \varepsilon_l(0, t) - q_l^{\text{on}}(t) \varepsilon_l^{\text{on}}(t), \quad j \in \mathcal{J}.$$

The entrance of EVs into the road network via junction j , entering links $l \in \mathcal{L}_j^+$, is described exogenously, through its on-ramp flow $q_l^{\text{on}}(t)$ and SoC $\varepsilon_l^{\text{on}}(t)$. Conversely, the exit of EVs from the road network via junction j , is defined by its off-ramp flow $q_l^{\text{off}}(t)$ and SoC $\varepsilon_l^{\text{off}}(t)$, $l \in \mathcal{L}_j^-$, which are a function of the EV traffic state at the downstream boundary of their respective links l , $\rho(X_l, t)$ and $\varepsilon(X_l, t)$.

In this work, we consider two types of junctions: interchanges and junctions connected to charging stations. At interchanges, we have multiple links entering and exiting the junction, and on- and off- ramps connecting the system with the *outside world*. A portion of the flow reaching the interchange junction on each link $l^- \in \mathcal{L}_j^-$, defined by the constant splitting ratio β_j , exits the system via the off-ramp,

$$q_{l^-}^{\text{off}}(t) = \beta_j q_{l^-}(X_{l^-}, t), \quad \varepsilon_{l^-}^{\text{off}}(t) = \varepsilon_{l^-}(X_{l^-}, t),$$

and the remainder is distributed to links $l^+ \in \mathcal{L}_j^+$,

$$q_{l^+}(0, t) = (1 - \beta_j) \sum_{i \in \mathcal{L}_j^-} q_i(X_i, t) \lambda_i^{\downarrow}(t),$$

$$q_{l^+}(0, t) \varepsilon_{l^+}(0, t) = (1 - \beta_j) \sum_{i \in \mathcal{L}_j^-} q_i(X_i, t) \varepsilon_i(X_i, t) \lambda_i^{\downarrow}(t).$$

Splitting ratios $\lambda_i^{\downarrow}(t)$ are the result of the EV routing decisions which will be discussed at the end of this section.

At junctions connected to charging stations, we have a single link entering and a single link leaving, and the on- and off-ramp flows connect the road network to a charging station, serving as a link between the two parts of the CTEC model. These flows, as well as other EV decisions related to charging stations, will be discussed next.

B. Charging station model

The state of each charging station $\zeta \in \mathcal{Z}$ is defined by the concentration of EVs present at different levels of SoC $\eta_\zeta(\varepsilon, t)$. The evolution of $\eta_\zeta(\varepsilon, t)$ is given by

$$\frac{\partial \eta_\zeta(\varepsilon, t)}{\partial t} + \frac{\partial (c_\zeta(\varepsilon, t) \eta_\zeta(\varepsilon, t))}{\partial \varepsilon} = \mu_\zeta^{\text{in}}(\varepsilon, t) - \mu_\zeta^{\text{out}}(\varepsilon, t),$$

where $c_\zeta(\varepsilon, t)$ denotes the rate at which the EVs are charging, $\mu_\zeta^{\text{in}}(\varepsilon, t)$ denotes the flow of EVs entering the charging station, and $\mu_\zeta^{\text{out}}(\varepsilon, t)$ the flow of EVs exiting it. These flows are defined as a function of the on- and off-ramp flows of the junction ζ connected to the charging station ζ ,

$$\mu_\zeta^{\text{in}}(\varepsilon, t) = \sum_{l \in \mathcal{L}_\zeta^-} \delta(\varepsilon - \varepsilon_l^{\text{off}}(t)) q_l^{\text{off}}(t),$$

where $\delta(x)$ is the Dirac delta function, and we have

$$q_\zeta^{\text{on}}(t) = \int_0^1 \mu_\zeta^{\text{out}}(\varepsilon, t) d\varepsilon, \quad q_\zeta^{\text{on}}(t) \varepsilon_\zeta^{\text{on}} = \int_0^1 \varepsilon \mu_\zeta^{\text{out}}(\varepsilon, t) d\varepsilon.$$

The power consumption of charging station ζ is defined as

$$P_\zeta(t) = \int_0^1 c_\zeta(\varepsilon, t) \eta_\zeta(\varepsilon, t) E d\varepsilon,$$

where E denotes the average capacity of EV batteries.

For each charging station $\zeta \in \mathcal{Z}$, we define the minimum, nominal, and maximum charging rate \underline{C}_ζ , \tilde{C}_ζ , and \overline{C}_ζ , respectively, $\underline{C}_\zeta \leq 0 \leq \tilde{C}_\zeta \leq \overline{C}_\zeta$. In order to make the charging station more appealing to the EVs, we guarantee that they will be charged at least at the nominal rate \tilde{C}_ζ until they reach some limit SoC $\tilde{\varepsilon}$. To this end, we split the vehicles present at charging station ζ into those with *low* SoC ($\varepsilon < \tilde{\varepsilon}$), and those with *high* SoC ($\varepsilon \geq \tilde{\varepsilon}$). The numbers of EVs of these two groups are

$$\eta_\zeta^{\text{lo}}(t) = \int_0^{\tilde{\varepsilon}} \eta_\zeta(\varepsilon, t) d\varepsilon, \quad \eta_\zeta^{\text{hi}}(t) = \int_{\tilde{\varepsilon}}^1 \eta_\zeta(\varepsilon, t) d\varepsilon,$$

respectively, jointly written as $N_\zeta(t) = [\eta_\zeta^{\text{lo}}(t) \ \eta_\zeta^{\text{hi}}(t)]^\top$. The charging rates are thus given by

$$c_\zeta(\varepsilon, t) = \begin{cases} \max\{0, c_\zeta^{\text{lo}}(t)\}, & \varepsilon = 0, \\ c_\zeta^{\text{lo}}(t), & 0 < \varepsilon < \tilde{\varepsilon}, \\ c_\zeta^{\text{hi}}(t), & \tilde{\varepsilon} \leq \varepsilon < 1, \\ \min\{0, c_\zeta^{\text{hi}}(t)\}, & \varepsilon = 1. \end{cases}$$

Group charging rates take values in $\tilde{C}_\zeta \leq c_\zeta^{\text{lo}}(t) \leq \overline{C}_\zeta$ and $\underline{C}_\zeta \leq c_\zeta^{\text{hi}}(t) \leq \overline{C}_\zeta$, and are given by a heuristic similar to the one in [5], prioritizing charging the *low* SoC vehicles,

$$c_\zeta^{\text{lo}}(t) = \begin{cases} \tilde{C}_\zeta, & P_\zeta^*(t) < \tilde{P}_\zeta(t), \\ \max\left\{\tilde{C}_\zeta, \min\left\{\frac{P_\zeta^*(t) - \eta_\zeta^{\text{hi}}(t)\tilde{C}_\zeta E}{\eta_\zeta^{\text{lo}}(t)E}, \overline{C}_\zeta\right\}\right\}, & P_\zeta^*(t) \geq \tilde{P}_\zeta(t), \end{cases}$$

$$c_\zeta^{\text{hi}}(t) = \begin{cases} \max\left\{\underline{C}_\zeta, \min\left\{\frac{P_\zeta^*(t) - \eta_\zeta^{\text{lo}}(t)\tilde{C}_\zeta E}{\eta_\zeta^{\text{hi}}(t)E}, \tilde{C}_\zeta\right\}\right\}, & P_\zeta^*(t) < \tilde{P}_\zeta(t), \\ \min\left\{\overline{C}_\zeta, \max\left\{\frac{P_\zeta^*(t) - \eta_\zeta^{\text{lo}}(t)\tilde{C}_\zeta E}{\eta_\zeta^{\text{hi}}(t)E}, \tilde{C}_\zeta\right\}\right\}, & P_\zeta^*(t) \geq \tilde{P}_\zeta(t), \end{cases}$$

where $P_\zeta^*(t)$ is the reference power (1) provided by the grid operator to the charging station ζ . Using thus defined $c_\zeta(\varepsilon, t)$ and assuming $\eta_\zeta(1, t) = 0$, the minimum, nominal, and maximum charging station power are defined as

$$\underline{P}_\zeta(t) = E[\underline{C}_\zeta \ \underline{C}_\zeta] N_\zeta(t), \quad (2)$$

$$\tilde{P}_\zeta(t) = E\tilde{C}_\zeta \mathbf{1}^\top N_\zeta(t), \quad (3)$$

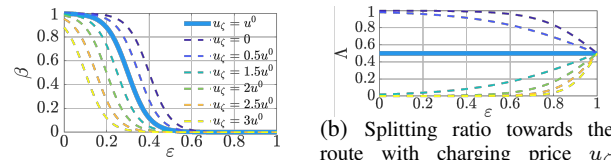
$$\overline{P}_\zeta(t) = E\overline{C}_\zeta \mathbf{1}^\top N_\zeta(t), \quad (4)$$

respectively, where $\mathbf{1}$ is a column vector of all 1-s of appropriate dimension. It can be verified that for $P_\zeta^*(t) = \tilde{P}_\zeta(t)$ we have $c_\zeta^{\text{lo}}(t) = c_\zeta^{\text{hi}}(t) = \tilde{C}_\zeta$. However, if $R_\zeta^\dagger(t) \neq 0$, it is possible that the charging station ζ violates its FCR commitments when $P_\zeta^*(t) < \underline{P}_\zeta(t)$ or $P_\zeta^*(t) > \overline{P}_\zeta(t)$, due to the limitations on $c_\zeta^{\text{lo}}(t)$ and $c_\zeta^{\text{hi}}(t)$.

C. EV decisions model

The model is completed by describing the aggregate influence of the EVs' decisions on when to enter the charging station, and which route to take, through defining the relevant splitting ratios based on the current EVs' SoC, traffic conditions, and price of charging of different charging stations. We adopt three modelling assumptions:

- Lower SoC makes the EVs more likely to enter the charging station.
- Higher charging price makes the EVs less likely to enter the charging station.
- EVs with a low SoC are more likely to go to the charging station with a lower price if given a choice.



(a) Splitting ratio towards the charging station with price u_c .

(b) Splitting ratio towards the route with charging price u_c assuming the only other route has charging price u_0 .

Fig. 2: Influence of charging price u_c on the splitting ratios.

Since human behaviour is notoriously difficult to model, in this work we propose and use simple behavioural heuristic, which enable us to analyse the system while still respecting the three stated assumptions. The dependence of the relevant splitting ratios on the charging price is illustrated in Fig. 2.

As EVs reach the charging station ζ on link $l \in \mathcal{L}_\zeta^-$, they have to make a decision on whether to enter it and charge, or continue driving and defer charging. We assume this decision depends only on their current SoC $\varepsilon_l(X_l, t)$ and the current charging price $u_\zeta(t)$. The outcome is modelled through the splitting ratio towards the charging station

$$\beta_\zeta(\varepsilon_l(X_l, t), u_\zeta(t)) = 1 - \left(1 + e^{-\frac{\varepsilon_l(X_l, t) - (U_0 + U_1 u_\zeta(t))}{\gamma_\zeta}}\right)^{-1},$$

where γ_ζ is a scaling constant, $U_0 + U_1 u_\zeta(t)$ is the threshold SoC indicating the level below which vehicles are more likely than not to enter the charging station, and U_0 and U_1 are constant parameters. Since the number of vehicles entering the charging station is expected to decrease as the charging price increases, we have $U_1 < 0$. For simplicity, we assume EVs decide to leave the charging station as soon as they are fully charged,

$$\mu_\zeta^{\text{out}}(\varepsilon, t) = \delta(\varepsilon - (1-))c_\zeta(\varepsilon, t)\eta_\zeta(\varepsilon, t),$$

where $1-$ indicates a point arbitrarily close to 1 from the left, yielding $q_\zeta^{\text{on}}(t) = c_\zeta^{\text{hi}}(t)\eta_\zeta(1-, t)$ and $\varepsilon_\zeta^{\text{on}}(t) = 1$.

Finally, EVs need to decide what route to take when they reach an interchange. We associate a score

$$\Lambda_{l^-}^{l^+}(t) = w_\theta \theta_{l^+}(t) + w_u (1 - \varepsilon_{l^-}(X_{l^-}, t))u_{\zeta_{l^+}}(t),$$

with each link $l^+ \in \mathcal{L}_j^+$ exiting the interchange, indicating its overall desirability to EVs approaching from link $l^- \in \mathcal{L}_j^-$, which is used to determine their splitting ratio towards it. Here, $\theta_{l^+}(t)$ denotes the travel time of link l^+ at time t , $u_{\zeta_{l^+}}(t)$ is the charging price of charging station ζ_{l^+} connected to link l^+ , and $w_\theta < 0$ and $w_u < 0$ are the constant weights of the two terms. Therefore, following [9], the splitting ratio of EVs arriving via link l^- towards link l^+ is given by

$$\lambda_{l^-}^{l^+}(t) = \frac{e^{\Lambda_{l^-}^{l^+}(t)}}{\sum_{i \in \mathcal{L}_j^+} e^{\Lambda_{l^-}^i(t)}}. \quad (5)$$

IV. CONTROL DESIGN

In this section we propose control laws for charging station ζ using the charging price $u_\zeta(t)$ to maximize its profit, while respecting its FCR commitments

$$\tilde{P}_\zeta(t) - \underline{P}_\zeta(t) \geq \mathcal{P}_\zeta^\dagger(t), \quad (6)$$

$$\overline{P}_\zeta(t) - \tilde{P}_\zeta(t) \geq \mathcal{P}_\zeta^\dagger(t). \quad (7)$$

We first linearize the model, then give a simple control law based on satisfying the FCR commitments, and finally introduce a prediction-based optimal pricing control law.

A. Model linearization

Due to the high complexity of the model, as well as the inherent uncertainty related to the decisions of the EVs and other charging stations, it is hard to find the required predictions of $N_\zeta(t)$ for $kT < t \leq (k+1)T$. Instead, a simplified linearized model is used for control design.

Considering the charging station model presented in Section III-B, the evolution of $N_\zeta(t)$ are approximated as

$$\dot{N}_\zeta(t) \approx AN_\zeta(t) + B\hat{\mu}_\zeta^{\text{in}}(t),$$

$$A = \begin{bmatrix} -\frac{\bar{C}}{\bar{\varepsilon}-\hat{\varepsilon}} & 0 \\ \frac{\bar{C}}{\bar{\varepsilon}-\hat{\varepsilon}} & -\frac{\bar{C}}{1-\hat{\varepsilon}} \end{bmatrix}, \quad B = \begin{bmatrix} 1 \\ 0 \end{bmatrix},$$

where $\hat{\varepsilon}$ is the average SoC of the EVs entering the charging station. The EV inflow to charging station ζ can be written

$$\hat{\mu}_\zeta^{\text{in}}(t) = \Delta_\zeta(t) + M_\zeta(t)u_\zeta(t), \quad (8)$$

where $u_\zeta(t)$ is the charging price, and $\Delta_\zeta(t) > 0$ contains the disturbance originating from model linearization errors and uncertainty about the traffic conditions. We represent the influence that an increase in price $u_\zeta(t)$ has on the inflow of EVs to the charging station, depending on the situation in the rest of the system, by $M_\zeta(t) \leq 0$. Due to the nature of the system, and piecewise-constant $u_\zeta(t) = u_\zeta(kT)$, $kT < t \leq (k+1)T$, it is enough to predict $N_\zeta(t)$ at the end of the control interval, $N_\zeta((k+1)T)$, which approximates to $N_\zeta((k+1)T) \approx e^{AT}N_\zeta(kT) + \hat{A}_T B(\Delta_\zeta(k) + M_\zeta(k)u_\zeta(kT))$, (9) where $\Delta_\zeta(k) = \frac{1}{T} \int_{kT}^{(k+1)T} \Delta_\zeta(t) dt$, $M_\zeta(k) = \frac{1}{T} \int_{kT}^{(k+1)T} M_\zeta(t) dt$, and $\hat{A}_T = \int_0^T e^{At} dt = A^{-1}(e^{AT} - I)$.

Finally, we need to determine the parameters of the inflow of EVs to each charging station $\zeta \in \mathcal{Z}$, $\Delta_\zeta(k)$ and $M_\zeta(k)$. The total EV flow entering charging station ζ , (8), is written

$$\hat{\mu}_\zeta^{\text{in}}(kT+\tau) = \sum_{l \in \mathcal{L}_\zeta^-} q_l(X_l, kT+\tau) \beta_\zeta(\varepsilon_l(X_l, kT+\tau), u_\zeta(kT)),$$

for $0 \leq \tau < T$, where \mathcal{L}_ζ^- is the set of all links from which EVs enter charging station ζ . This expression can be simplified in steady state, where we assume the EVs traverse these links at a constant speed, $v_l(x, t) = \frac{X_l}{\theta_l(t)}$, that the total traffic flow circulating in the network is approximately constant, $\sum_{\zeta \in \mathcal{Z}} \sum_{l \in \mathcal{L}_\zeta^-} q_l(0, t) \approx \hat{q}$, and that the SoC of EVs arriving at the charging stations is approximately constant, $\varepsilon_l(X_l, t) \approx \hat{\varepsilon}$. In this case, we may approximate the total number of EVs that enters charging station ζ during $kT \leq t < (k+1)T$ as

$$\hat{\mu}_\zeta^{\text{in}}(k) \approx \beta_\zeta(\hat{\varepsilon}, u_\zeta(kT)) \left((T - \hat{\theta}_\zeta(k)) \hat{\lambda}_\zeta(k) + \hat{\theta}_\zeta(k) \hat{\lambda}_\zeta(k-1) \right) \hat{q}, \quad (10)$$

where $\hat{\theta}_\zeta(k)$ is the average travel time from the interchanges to the charging station ζ at time $t = kT$, and $\hat{\lambda}_\zeta(k)$ is

$$\hat{\lambda}_\zeta(k) = \frac{e^{w_\theta \hat{\theta}_\zeta(k) + w_u(1-\hat{\varepsilon})u_\zeta(kT)}}{\sum_{i \in \mathcal{Z}} e^{w_\theta \hat{\theta}_i(k) + w_u(1-\hat{\varepsilon})u_i(kT)}},$$

which is a special case of the routing decision model (5). Note that $\hat{\mu}_\zeta^{\text{in}}(k)$ therefore depends not only on $u_\zeta(kT)$, but also on the charging price of other charging stations. Finally, we linearize (10) around $u_\zeta(kT) \approx \hat{u}_\zeta(k)$, $\zeta \in \mathcal{Z}$, yielding

$$\underline{M}(k) = \left(\frac{\partial \hat{\mu}_\zeta^{\text{in}}(k)}{\partial u_\zeta(kT)} \right) \Big|_{u_\zeta(kT) = \hat{u}_\zeta(k), \zeta \in \mathcal{Z}},$$

$$\underline{\Delta}(k) = \left(\hat{\mu}_\zeta^{\text{in}}(k) - \underline{M}(k)u_\zeta(kT) \right) \Big|_{u_\zeta(kT) = \hat{u}_\zeta(k), \zeta \in \mathcal{Z}}.$$

The choice of the linearization prices $\hat{u}_\zeta(k)$ has a significant impact on the quality of inflow prediction. Since charging station ζ does not know what the next charging price of other charging stations will be, we linearize $\hat{\mu}_\zeta^{\text{in}}(k)$ around

$$\hat{u}_\zeta(k) = \alpha_u u_\zeta((k-1)T), \quad \zeta \in \mathcal{Z},$$

where $0 < \alpha_u < 1$. We improve robustness by selecting a lower α_u , adopt the pessimistic assumption that the charging stations will reduce their price for the coming hour, thus making it harder for charging station ζ to attract EVs.

B. Commitment-satisfaction control

Having linearized the model, we are now able to propose a simple control law which uses feedforward to satisfy constraints (6) and (7), and feedback to suppress the effect of variations in the aggregate disturbance $\Delta(t)$. Substituting (2), (3), (4), and (9) into (6) and (7), and assuming $\underline{\Delta}(t) = 0$, these constraints can be approximated to

$$\left(\bar{C}_\zeta - \underline{C}_\zeta \right) E [0 \quad 1] \left(e^{AT} N_\zeta(kT) + \hat{A}_T B \hat{\mu}_\zeta^{\text{in}}(kT) \right) \geq \underline{P}_\zeta^\uparrow(k),$$

$$\left(\bar{C}_\zeta - \underline{C}_\zeta \right) E \mathbb{1}^\top \left(e^{AT} N_\zeta(kT) + \hat{A}_T B \hat{\mu}_\zeta^{\text{in}}(kT) \right) \geq \bar{P}_\zeta^\downarrow(k).$$

Here, $\underline{P}_\zeta^\uparrow(k)$ and $\bar{P}_\zeta^\downarrow(k)$ are the more stringent constraints between those at kT and $(k+1)T$,

$$\underline{P}_\zeta^\uparrow(k) = \alpha_P \min \left\{ \underline{P}_\zeta^\uparrow(kT), \underline{P}_\zeta^\uparrow((k+1)T) \right\},$$

$$\bar{P}_\zeta^\downarrow(k) = \alpha_P \max \left\{ \bar{P}_\zeta^\downarrow(kT), \bar{P}_\zeta^\downarrow((k+1)T) \right\},$$

multiplied by some constant $\alpha_P > 1$ to improve robustness to disturbance by tightening the constraints.

Both of these constraints are satisfied if $u_\zeta(kT)$ is chosen such that $\hat{\mu}_\zeta^{\text{in}}(kT) \geq \hat{\mu}_\zeta^{\text{in}\downarrow}(k)$, where

$$\hat{\mu}_\zeta^{\text{in}\downarrow}(k) = \max \left\{ \hat{\mu}_\zeta^{\text{in}\uparrow}(k), \hat{\mu}_\zeta^{\text{in}\downarrow}(k) \right\}, \quad (11)$$

and $\hat{\mu}_\zeta^{\text{in}\uparrow}(k)$ and $\hat{\mu}_\zeta^{\text{in}\downarrow}(k)$ are the minimum inflows to charging station ζ that will cause constraints (6) and (7) to be satisfied, respectively

$$\hat{\mu}_\zeta^{\text{in}\uparrow}(k) = \frac{\underline{P}_\zeta^\uparrow(k)}{(\bar{C}_\zeta - \underline{C}_\zeta)E} - [0 \quad 1] e^{AT} N_\zeta(kT),$$

$$\hat{\mu}_\zeta^{\text{in}\downarrow}(k) = \frac{\bar{P}_\zeta^\downarrow(k)}{(\bar{C}_\zeta - \underline{C}_\zeta)E} - \mathbb{1}^\top e^{AT} N_\zeta(kT).$$

Finally, the commitment-satisfaction control law is given by

$$u_\zeta(kT) = \frac{1}{\underline{M}_\zeta(k)} \left(\hat{\mu}_\zeta^{\text{in}\downarrow}(k) - \underline{\Delta}_\zeta(k) \right).$$

C. Optimal pricing control

At every time $t = kT$, the optimal pricing control law aims to calculate the updated charging price for the next interval, $u_\zeta(kT)$, so that the profit of charging station is maximized and so that it respects its FCR commitments. This is achieved by solving the maximization problem

$$\begin{aligned} & \max_{u_\zeta(kT)} J_\zeta(k) \\ & \text{s.t. model dynamics} \\ & \text{FCR capacity commitments} \\ & \mathbb{1}^\top N_\zeta(t) \leq \bar{N}_\zeta \\ & kT < t \leq (k+1)T \end{aligned} \quad (12)$$

with $J_\zeta(k)$ reflecting the hourly profit of charging station ζ ,

$$J_\zeta(k) = (u_\zeta(kT) - \pi(k)) \int_{kT}^{(k+1)T} \tilde{P}_\zeta(t) dt, \quad (13)$$

where $\pi(k)$ is the price of electricity for $kT \leq t < (k+1)T$.

Following the discussion from the previous section, constraints (6) and (7) can be rewritten as constraints on the charging price $u_\zeta(kT)$

$$u_\zeta(kT) \leq \frac{1}{M_\zeta(k)} \left(\hat{\mu}_\zeta^{\text{in}\dagger}(k) - \underline{\Delta}_\zeta(k) \right),$$

where $\hat{\mu}_\zeta^{\text{in}\dagger}(k)$ is the more restrictive minimum inflow (11). Similarly, constraint (12) can be rewritten as

$$\mathbf{1}^\top \left(e^{AT} N_\zeta(kT) + \hat{A}_T B(\underline{\Delta}_\zeta(k) + M_\zeta(k) u_\zeta(kT)) \right) \leq \bar{N}_\zeta.$$

Since the nominal power $\tilde{P}_\zeta(t)$ depends directly on $N_\zeta(t)$ according to (3), considering (9) we have

$$\int_{kT}^{(k+1)T} N_\zeta(t) dt \approx \hat{A}_T N_\zeta(kT) + A^{-1} (\hat{A}_T - TI) B(\underline{\Delta}_\zeta(k) + M_\zeta(k) u_\zeta(kT)),$$

and therefore cost function (13) can be approximated by

$$J'_\zeta(k) = \alpha_2(k) u_\zeta^2(kT) + \alpha_1(k) u_\zeta(kT) \approx J_\zeta(k),$$

where the current coefficients $\alpha_1(k)$ and $\alpha_2(k)$ are

$$\alpha_1(k) = \mathbf{1}^\top \left(\hat{A}_T N_\zeta(kT) + A^{-1} (\hat{A}_T - TI) B(\underline{\Delta}_\zeta(k) - M_\zeta(k) \pi(k)) \right),$$

$$\alpha_2(k) = \mathbf{1}^\top A^{-1} (\hat{A}_T - TI) B M_\zeta(k).$$

The optimization problem can thus be approximated by

$$\begin{aligned} \max_{u_\zeta(kT)} \quad & \alpha_2(k) u_\zeta^2(kT) + \alpha_1(k) u_\zeta(kT) \\ \text{s.t.} \quad & u_\zeta(kT) \leq \frac{1}{M(k)} \left(\min\{\hat{\mu}_\zeta^{\text{in}\dagger}(k), \hat{\mu}_\zeta^{\text{in}\downarrow}(k)\} - \underline{\Delta}(k) \right) \\ & u_\zeta(kT) \geq \frac{1}{M(k)} \left(\frac{\bar{N}_\zeta - \mathbf{1}^\top e^{AT} N_\zeta(kT)}{\mathbf{1}^\top \hat{A}_T B} - \underline{\Delta}(k) \right) \end{aligned}$$

It can be shown that $\alpha_2(k) < 0$, yielding a convex problem.

V. SIMULATION RESULTS

Finally, we test the proposed charging station pricing control laws for providing balancing services, in simulations of the set-up outlined in Section II and Figure 1. The main simulation parameters are given in Table I.

The considered road network consists of 8 junctions, of which 2 interchanges and 6 charging station off-ramps, with 3 routes connecting the 2 interchanges (j_1 and j_2) in both directions, formed of 12 links (4 links per route, $j_1 \rightarrow \zeta_i$, $\zeta_i \rightarrow j_2$, $j_2 \rightarrow \zeta_i$, and $\zeta_i \rightarrow j_1$). Formally, there are 6 charging stations, but the pairs of virtual charging stations associated to each route are considered jointly as one charging station.

The simulation model is initialized with uniformly distributed initial traffic density $\rho_l(x, 0) \in [6, 13.5]$ veh/km, uniformly distributed initial SoC $\varepsilon_l(x, 0) \in [0.4, 0.6]$, and

Symbol	Value	Unit	Symbol	Value	Unit
X_l	25	km	U_0	0.4	1
T	1	h	U_1	-0.0125	1/EUR
E	60	kWh	w_θ	-36	1/h
\bar{C}_ζ	-0.83	1/h	w_u	-1	1/EUR
\underline{C}_ζ	0.83	1/h	$\hat{\varepsilon}$	0.45	1
\bar{C}_ζ	1.67	1/h	\hat{q}	4600	veh/h
\bar{N}_ζ	50	veh	α_u	0.8	1
$\hat{\varepsilon}$	0.7	1	α_P	1.2	1

TABLE I: Simulation parameters and their values.

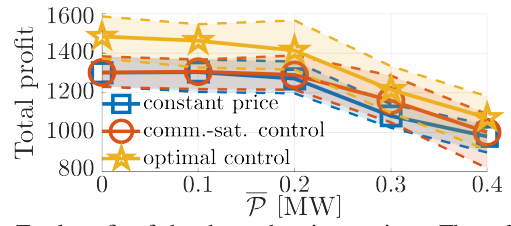


Fig. 3: Total profit of the three charging stations. The solid lines show the median profits over all simulation runs, and the range between the first and third quartile is shaded and outlined dashed.

$\eta_\zeta(\varepsilon, 0) = 0$ veh. The dynamics of EV traffic are described by an exponential traffic speed function

$$V(\rho) = v_{\text{ff}} e^{-\frac{1}{2} \left(\frac{\rho}{\rho_{\text{cr}}} \right)^2}$$

with $v_{\text{ff}} = 100$ km/h, $\rho_{\text{cr}} = 15$ veh/km, and a second-order polynomial battery discharge function

$$D(v) = D_0 + D_1 v + D_2 v^2$$

with parameters $D_0 = 0.0175$ 1/h, $D_1 = 3 \cdot 10^{-3}$ 1/km, and $D_2 = 2.15 \cdot 10^{-5}$ h/km². The system is initialized by keeping all charging prices constant and balancing capacities at zero for the first two hours.

Charging stations with three different pricing strategies are competing against each other:

- 1) Constant price, not providing FCR
- 2) Commitment-satisfaction controlled price, providing FCR
- 3) Optimally controlled price, providing FCR

The second control schemes is described in Section IV-B, and the third in Section IV-C. The hourly committed balancing capacities of both charging stations are randomly generated day-ahead, with uniformly distributed $\mathcal{P}_\zeta^\dagger(kT) \sim \mathcal{U}[0, \bar{P}]$ MW and $\mathcal{P}_\zeta^\ddagger(kT) \sim \mathcal{U}[-\bar{P}, 0]$ MW. The charging stations' FCR are activated at random times, generated as a Poisson arrival process with an average gap of 1 h, and it is equally likely that the request is for upward (with $R_\zeta^\ddagger(t) < 0$) and for downward ($R_\zeta^\dagger(t) > 0$) regulation. The hourly price at which the charging stations buy electricity $\pi(kT) \sim \mathcal{U}[4, 10]$ is known ahead of time.

We executed five simulation batches, with 100 runs of 24 hours each, using different maximum balancing capacity commitments $\bar{P} \in \{0, 0.1, 0.2, 0.3, 0.4\}$ MW. The results are shown in Fig. 3, displaying the total profit statistics achieved by different charging stations. Since the commitment-satisfaction price control law is designed solely to ensure that the balancing capacity commitments are respected, its charging price is set to the same nominal value as that of the first one for $\bar{P} = 0$ MW and $\bar{P} = 0.1$ MW.

It can be seen from Fig. 3 that the profit of all charging stations decreases as \bar{P} increases, requiring more competitive pricing to ensure that the balancing commitments are satisfied. This holds even for the charging station with constant price and no commitments, since the other two charging stations will need to reduce their prices in order to attract enough EVs. Note that in this case the FCR revenues are not included, hence the total achieved profit will be higher. The optimally priced charging station consistently achieves the best profit, but in case of $\bar{P} = 0.4$ MW, it does slightly violate the balancing commitments, with

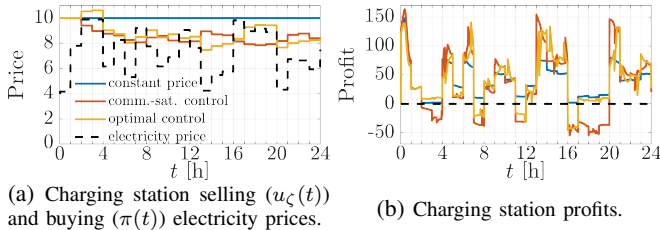


Fig. 4: Charging station prices and profits.

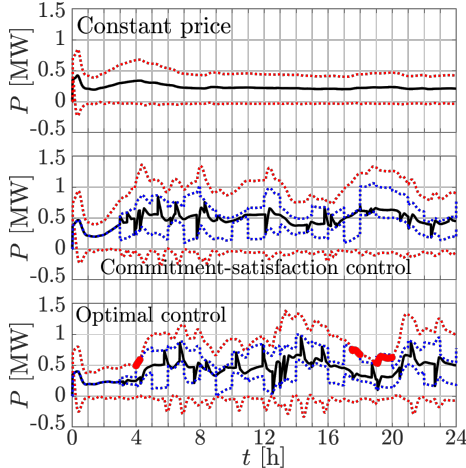


Fig. 5: Current charging station power $P_c(t)$ (black), maximum ($P_c^+(t)$) and minimum ($P_c^-(t)$) achievable power (dotted red), and committed range of reference power for downward ($P_c^-(t) + P_c^{\downarrow}(t)$) and upward ($P_c^+(t) + P_c^{\uparrow}(t)$) regulation (dotted blue). Thick red line indicates times when the FCR commitment is violated.

average and maximum cumulative violation of 0.0711 MWh and 0.717 MWh, respectively, over all simulation runs. In practice, these violations could be offset using stationary storage, or by better selecting of balancing capacity commitments to match the expected EV traffic conditions.

In order to better demonstrate the operation of the model and the control laws, we display the details of one simulation run with $\bar{P} = 0.4$ MW. In Fig. 4 we show the charging and electricity prices, as well as charging station profits over time, and in Fig. 5 the evolution of charging station power over the course of the simulation run (with spikes due to the arrival of FCR requests). As shown in Fig. 5 (bottom), the optimal pricing control does violate the balancing capacity commitments, but in practice, this violation is very small, with total energy of 0.2629 MWh. As a result of lower conservatism, allowing higher charging prices, the optimal pricing control achieves around 20% higher profit than the commitment-satisfaction control in this case.

VI. CONCLUSIONS

In this work we proposed a framework for EV charging station pricing control for maximizing their profit, while ensuring they can provide FCR. We extended the CTEC model to the case of the road network, as well as to explicitly capture the influence of the charging price on EV decisions, and designed the pricing control laws based on the linearized model. Charging stations with different control laws are made to compete against each other in the

simulations, and are in general shown to be able to respect their balancing capacity commitments, while achieving better profit than the benchmark charging station with constant charging price. It was shown that the FCR commitments by the charging stations requires them to reduce their charging price, potentially leading to cheaper service for the consumers, while also helping the power grid.

In the future, all facets of the overall system will need to be considered in more detail. The dynamics of the EV traffic and the influence that the altered routing behaviour will have on it is among the topics that need to be addressed. On the other side, a more realistic representation of the power grid and its complexities will need to be considered explicitly. Finally, practical aspects of implementing FCR via EV charging stations need to be tackled, and the potential contribution of such schemes to building a more sustainable future need to be assessed.

REFERENCES

- [1] G. Conway, A. Joshi, F. Leach, A. García, and P. K. Senecal, "A review of current and future powertrain technologies and trends in 2020," *Transportation Engineering*, vol. 5, p. 100 080, 2021.
- [2] M. Esteban, J. Portugal-Pereira, B. C. McLellan, *et al.*, "100% renewable energy system in japan: Smoothing and ancillary services," *Applied energy*, vol. 224, pp. 698–707, 2018.
- [3] A. Oudalov, D. Chartouni, and C. Ohler, "Optimizing a battery energy storage system for primary frequency control," *IEEE Transactions on power systems*, vol. 22, no. 3, pp. 1259–1266, 2007.
- [4] P. H. Divshali and C. Evens, "Optimum day-ahead bidding profiles of electrical vehicle charging stations in fcr markets," *Electric Power Systems Research*, vol. 190, p. 106 667, 2021.
- [5] M. Čičić, C. Vivas, C. Canudas-de-Wit, and F. R. Rubio, "Optimal renewable energy curtailment minimization control using a combined electromobility and grid model," in *IFAC World Congress*, 2023.
- [6] M. Fochesato, C. Cenedese, and J. Lygeros, "A Stackelberg game for incentive-based demand response in energy markets," in *2022 IEEE 61st Conference on Decision and Control (CDC)*, IEEE, 2022, pp. 2487–2492.
- [7] S. Wang, S. Bi, and Y. A. Zhang, "Reinforcement learning for real-time pricing and scheduling control in ev charging stations," *IEEE Transactions on Industrial Informatics*, vol. 17, no. 2, pp. 849–859, 2019.
- [8] D. Ban, G. Michailidis, and M. Devetsikiotis, "Demand response control for phev charging stations by dynamic price adjustments," in *2012 IEEE PES Innovative Smart Grid Technologies (ISGT)*, IEEE, 2012, pp. 1–8.
- [9] M. E. Ben-Akiva, S. R. Lerman, and S. R. Lerman, *Discrete choice analysis: theory and application to travel demand*. MIT press, 1985, vol. 9.
- [10] B. Canizes, J. Soares, A. Costa, *et al.*, "Electric vehicles' user charging behaviour simulator for a smart city," *Energies*, vol. 12, no. 8, p. 1470, 2019.
- [11] L. Hu, J. Dong, and Z. Lin, "Modeling charging behavior of battery electric vehicle drivers: A cumulative prospect theory based approach," *Transportation Research Part C: Emerging Technologies*, vol. 102, pp. 474–489, 2019.
- [12] M. Čičić and C. Canudas-de-Wit, "Coupled macroscopic modelling of electric vehicle traffic and energy flows for electromobility control," in *2022 IEEE 61st Conference on Decision and Control (CDC)*, IEEE, 2022, pp. 826–831.